Photovoltaic Thermal Power Supply Based on Smart Grid Functioning Solar Electric System Network

Eugene Chaikovskaya*

Odessa Polytechnic National University, Ukraine

Abstract: Integrated Smart Grid systems are developed to coordinate the production and consumption of electricity from a grid-connected solar power plant, providing power to a heat pump and hot water using hybrid solar collectors. The upper section of a two-section storage tank supplies hot water, while the lower section is a low-grade energy source for the heat pump. The integrated dynamic subsystem of the solar power system includes the following components: the grid, photovoltaic solar panels, hybrid solar collectors, a grid-connected inverter, a heat pump, a two-section storage tank, and a frequency converter. The power factor and local water temperature of the grid-connected solar power system are predicted by measuring the voltage of the hybrid solar collectors at the grid-connected inverter input, the voltage at the frequency converter output, and the current frequency. Advanced solutions for varying the power of the heat pump compressor motor and the circulation pump motor are implemented in accordance with changes in the thermal output of the storage tanks connected to the hybrid solar collectors. The power of the heat pump compressor motor and the circulating pump motor is regulated based on the specified voltage ratio at the grid-tie inverter input from the hybrid solar collectors and at the frequency converter output. The functional assessment of the solar power system power factor change when connecting the heat pump is in the range of 58–98%, when connecting the hot water supply, in the range of 63.74–98%, and the local water temperature in the range of 35–55°C. When the grid-tie inverter input voltage changes from 200 V to 600 V, the power transmitted to the grid increases in the range of 0.33 to 1, the power factor by 40%. Determining the final functional information allows for early decisions to be made about changing the operating mode of the heat pump compressor motor and the circulating motor to prevent peak loads on the power grid and maintain voltage in the distributed system.

Keywords: Solar energy, Smart grid, Hybrid solar collectors, Heat pamp power supply, Hot water power supply, Power factor.

1. INTRODUCTION

Distributed generation of electricity using renewable sources requires improvement of production and consumption coordination management technologies. A comprehensive integrated solar power plant system has been developed to support the operation of a biogas plant based on a heat pump, for which fermented wort is a low-potential energy source [1]. The change in the power factor of the solar power system connected to the grid and the temperature of the coolant entering the heat exchanger built into the methane tank are predicted. Promising solutions include changing the power of the heat pump compressor to maintain biogas production, unloading fermented wort and loading fresh material while maintaining the power factor of the grid solar system and changing the level of electricity transmission to the grid. The use of the developed Smart Grid technology allows preventing peak loads of the power system, reducing electricity consumption from the grid by up to 30%. Thus, the author [2] proposes to maintain voltage in the distribution system when using a solar grid power system based on integrated storage management. A comprehensive integrated system for supporting the operation of a grid solar power system has been developed based on forecasting changes in the storage capacity and the power factor of the grid solar power system. Promising solutions for changing the capacity of the thermoelectric storage device redistribute the accumulated electricity. Changing the level of electricity transmission to the grid allows maintaining voltage in the distribution system by maintaining the power factor of the grid solar power system. Peak load on the power system is prevented, which reduces energy consumption from the grid by up to 14%. In paper [3] a concentrating photovoltaic and temperature difference combined power generation device is designed. The device is guided by the problem of low power generation efficiency of solar cells at high temperature, and transfers the heat of photovoltaic cells to thermoelectric cells to achieve secondary power generation. The research takes the cold end of the thermoelectric battery as the entry point, and studies its influence on the device by controlling the flow rate and temperature of the cooling liquid in the water-cooled radiator. In [4] the integration of solar, wind, and battery sources into the main grid is presented, along with a control system that ensures energy flow from the hybrid system to the load and the main grid. The current and voltage regulator are optimized using a particle swarm optimization algorithm. This article [5] examines strategies for retrofitting solar spaces in traditional dwellings on the Qinghai-Tibet Plateau, focusing on increasing solar energy gains and addressing cultural heritage preservation concerns. The study aims to inform future

*Address correspondence to this author at the Odessa Polytechnic National University, Ukraine;
E-mail: eechaikovskaya@gmail.com

Received on 27-10-2025 Accepted on 02-12-2025 Published on 06-12-2025

E-ISSN: 2410-2199/25

retrofitting projects that balance improved thermal performance with preserving cultural integrity in this high-altitude region. This study[6] investigates the influence of solar peak energy and weather classification features on a Bidirectional Long Short-Term Memory (BiLSTM) model for multi-step Global Horizontal Irradiance (GHI) prediction. The practical implication of these results is that reliable irradiance forecasts can be achieved with simpler BiLSTM configurations, reducing computational cost and supporting real-time energy management, PV system sizing, and grid stability in equatorial regions. This paper [7] proposes a new power architecture that integrates a rechargeable lithium-ion battery and an intelligent power management system into the LED TV frame. This integrated solution eliminates the need for separate UPS systems, improves reliability, and enables future integration with renewable sources such as rooftop solar panels. In [8] the technical-economic viability of hybrid renewable energy systems that include personal electric vehicles (EVs) in the Middle East and North Africa (MENA) area is assessed in this study. The results show how the hybrid combination of photovoltaic with the grid provided the most significant configuration across the MENA region according to the sensitivity studies that indicate considerable potential for wider application. Eliminating subsidies and modifying power rates are two important tactics for promoting the use of hybrid renewable energy systems. For policymakers and investors in the MENA area, these studies provide practical insights. This study [9] summarizes the performance of a photovoltaic/thermal (PV/T) system integrated with a glass-to-PV backsheet (PVF film-based backsheet) and glass-to-glass photovoltaic (PV) cells protections. A dual-fluid heat exchanger is used to cool the PV cells in which water and air are operated simultaneously. The proposed PV/T design brings about a higher electric output while producing sufficient thermal energy. A detailed numerical study was performed by calculating real-time heat transfer coefficients. Energy balance equations across the dual-fluid PV/T system were solved using an ordinary differential equation (ODE) solver in MATLAB. In this paper [10], a hybrid PV/thermal(PV/T) water system is proposed to mitigate this problem. This system combines a PV panel and a thermal collector. An optimal linear quadratic regulator (LQR)is proposed to control the PV cell temperature around an optimal value that maximises electricity generation. Since the system model is nonlinear, an optimal LQR gain-scheduling state-feedback control approach based on an LPV representation of the nonlinear model is designed using the Linear Matrix Inequality (LMI) method. The goal is to obtain the maximum electrical power for each solar panel. Since a reduced number of sensors is available, an LPV Kalman filter is also proposed to estimate the system states required by the state-feedback controller.

A pressing challenge in the context of the further development of distributed energy is to coordinate the energy production and consumption of a grid-connected solar power system based on heat pumps and hot water supply using hybrid solar collectors. This is achieved through predictive solutions for regulating the power of the heat pump's compressor motor and the circulation pump motor in accordance with changes in the thermal output of a two-section storage tank connected to the hybrid solar collectors. The lower section is a source of low-grade energy for the heat pump, while the upper section provides hot water. The novelty of this work should be presented. Distributed power generation using renewable sources requires improved technologies for managing the coordination of production and consumption. Traditionally, voltage regulation in the electric grid is accomplished using, for example, transformers, capacitor banks, voltage regulators, static synchronous compensators, etc. The installation and maintenance costs of these devices can be quite high, and some have a relatively slow response time of around several seconds. The PVT system, as an element of the grid-tied solar power system, acquires the additional status of a voltage regulator in the distribution power system. Therefore, the change in the power factor of the grid-tied solar power system and the temperature of the heated water in for heat pump and hot water supply are predicted. A two-section storage tank connected to hybrid solar collectors for heat pump and hot water supply . The upper section is for hot water supply. The lower section serves as a source of low-potential energy for heat heat pump. Promising solutions include varying the power of the heat pump compressor motor and the circulation pump motor in accordance with the change in the thermal power of the storage tank sections while maintaining the power factor of the grid-tied solar system and changing the level of electricity transmission to the grid. The voltage at the input of the hybrid inverter from the hybrid solar collectors, the voltage at the output of the frequency converter to assess their ratio, and the voltage frequency are continuously measured. The specified voltage ratio is part of the K_t, K_{pf} coefficients of the transfer function (3) applied to complex mathematical modeling within the grid-tied solar power system. The result of complex modeling is a benchmark assessment of changes in the power factor and the temperature of the heated water. During operation of the electrical system, the established ratio of the voltage at the grid inverter input and the voltage at the frequency converter output changes, which are

measured. Therefore, performance monitoring was performed using a mathematical justification of the architecture, support for the functioning of the electrical system, and a transfer function. Logical modeling results in obtaining resulting information regarding proactive decisions to change the power of the heat pump electric motor, the circulation pump, and the transmission of electrical energy to the grid. The power factor and the temperature of the heated water are maintained. For this purpose, a comprehensive Smart Grid system for coordinating the production and consumption of a solar PVT electrical system was developed based on logical modeling. This means that the obtained scientific result in the form of a comprehensive Smart Grid system based on support for the power factor of the solar electric system and the temperature of the heated water is relevant, which makes it possible to solve problems using Smart Grid technologies to achieve the stability and reliability of energy systems in order to provide consumers with high-quality electricity in terms of energy conservation, progressive from a theoretical perspective. From a practical perspective, the developed integrated system allows us to determine the conditions for improving distributed energy generation technology to prevent peak loads on the power grid. Thus, the practical application of the obtained scientific results lies in the possibility of applying them to the development of intelligent Smart Grid systems using renewable energy sources. This creates the preconditions for the transfer of the resulting technological solutions. The objective of this study is to validate the operation of a grid-tied solar energy system using combined solar collectors to provide both heat pump power and hot water. Changes in the power factor and local water temperature are predicted. The voltage at the grid-tied inverter input from the hybrid solar panels, the voltage at the frequency converter output, and the voltage frequency are measured. The change in the ratio of the input voltage from the hybrid solar collectors at the grid-tied inverter input to the output voltage of the frequency converter is estimated. Predictive decisions are made to adjust the power of the heat pump compressor motor and the circulation pump motor in accordance with changes in the thermal output of a two-section storage tank connected to the hybrid solar collectors. The lower section is a low-potential energy source for the heat pump, while the upper section provides hot water. A grid-tied heating system is used to maintain water heating and regulate the level of energy transfer to the grid. To achieve this goal, the following objectives were set:

– develop a structural diagram and conduct comprehensive mathematical modeling to obtain a reference estimate of changes in the power factor and hot water temperature of a grid-connected solar power system;

– develop a structural diagram and conduct logical modeling to obtain a functional estimate of changes in the power factor and hot water temperature;

– develop a structural diagram and conduct logical modeling to obtain final information at the decision-making level for changing the power of the heat pump compressor motors and the circulation pump;

– develop a comprehensive system for coordinating electricity production and consumption based on forecasting changes in the power factor and hot water temperature of a grid-connected solar power plan.

2. PROPOSED METHOD

2.1. Methodological and Mathematical Substantiation

Based on the methodological, mathematical, logical substantiation of the technological systems [11] the architecture, mathematical substantiation of the architecture (1) are proposed (Figure **1**).

The mathematical substantiation of the architecture of the PVT electric system Smart Grid (1), (Figure **1**), based on the methodology of the mathematical description of dynamics of power systems, the method of the graph of cause-effect relations [11] is proposed. The integrated dynamic subsystem includes the following components: mains, photovoltaic solar panels, hybrid solar collectors, grid inverter, two-section storage tank, upper section for hot water supply, lower section as a low-grade energy source for heat pump , and frequency converter.

Where $PVTESSG(\tau)$ – PVT electric system Smart Grid; τ – time, seconds; $ID(\tau)$ – integrated dynamic subsystem (mains, photovoltaic solar panels, hybrid solar collectors, grid inverter, heat pump, two-section storage tank, upper section for hot water supply, lower section as a low-grade energy source for heat pump, frequency converter); $P(\tau)$ – properties of the components of the PVT electric system; $x(\tau)$ – impacts (change in solar radiation, change in consumption of electrical energy and heat; $f(\tau)$ – parameters that are measured: (voltage at the grid inverter input from hybrid solar collectors, voltage at the frequency converter output, current frequencies); $K(\tau)$ – coefficients of mathematical description of the dynamics of power factor of the PVT electric system, the local water temperature; $y(\tau, z)$ – predicted output

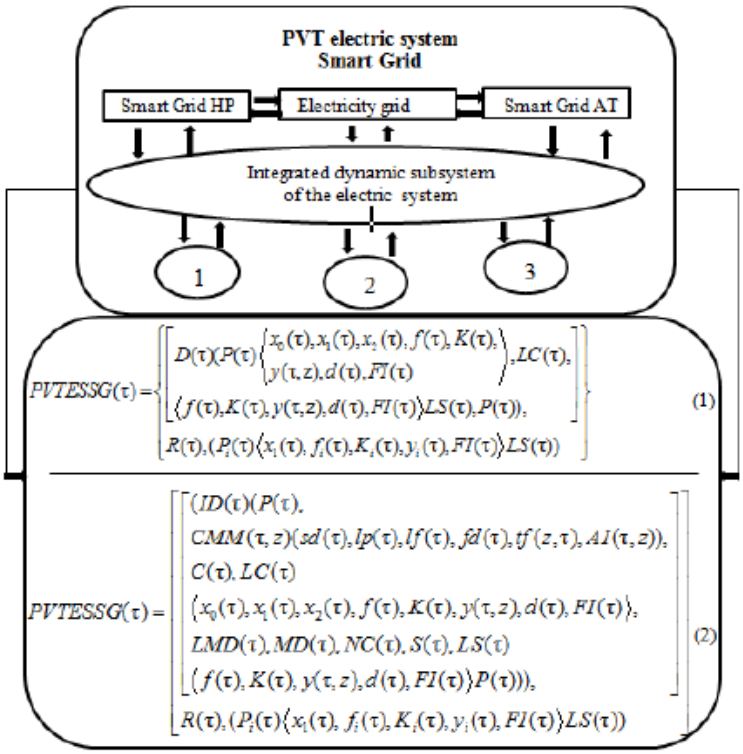

$$PVTESSG(\tau)=\left\{\begin{bmatrix} D(\tau)(P(\tau)\left\langle\begin{matrix}x_0(\tau),x_1(\tau),x_2(\tau),f(\tau),K(\tau),\\ y(\tau,z),d(\tau),FI(\tau)\end{matrix}\right\rangle,LC(\tau),\\ \left\langle f(\tau),K(\tau),y(\tau,z),d(\tau),FI(\tau)\right\rangle LS(\tau),P(\tau)),\\ R(\tau),(P_i(\tau)\left\langle x_i(\tau),f_i(\tau),K_i(\tau),y_i(\tau),FI(\tau)\right\rangle LS(\tau)) \end{bmatrix}\right\} \quad (1)$$

$$PVTESSG(\tau)=\left[\begin{bmatrix} (ID(\tau)(P(\tau),\\ CMM(\tau,z)(sd(\tau),lp(\tau),lf(\tau),fd(\tau),tf(z,\tau),AI(\tau,z)),\\ C(\tau),LC(\tau)\\ \left\langle x_0(\tau),x_1(\tau),x_2(\tau),f(\tau),K(\tau),y(\tau,z),d(\tau),FI(\tau)\right\rangle,\\ LMD(\tau),MD(\tau),NC(\tau),S(\tau),LS(\tau)\\ \left\langle f(\tau),K(\tau),y(\tau,z),d(\tau),FI(\tau)\right\rangle P(\tau))),\\ R(\tau),(P_i(\tau)\left\langle x_i(\tau),f_i(\tau),K_i(\tau),y_i(\tau),FI(\tau)\right\rangle LS(\tau)) \end{bmatrix}\right] \quad (2)$$

Figure 1: PVT electric system Smart Grid: the architecture: HP – heat pump; AT – accumulator tank; **1** – charging unit; **2** – discharging unit; **3** – unit for functional efficiency evaluation. Mathematical substantiation of the architecture (**1**). Mathematical substantiation of operational maintenance (**2**)

parameters (power factor, the local water temperature) *z* – spatial coordinate of the condenser axis, heat exchanger coincides with the direction of the flow of motion of the medium, metres; *d*(τ) – dynamic parameters of power factor change, the local water temperature change; *FI*(τ) – functional resulting information on decision-making; *LC*(τ) – logical relations regarding the operability control of the PVT electric system; *LS*(τ) – logical relations regarding the identification of the state of the PVT electric system; *R*(τ) – logical relations in *PVTESSG*(τ) to confirm the correctness of decisions made from the units of the PVT electric system. Indices: *i* – the number of elements of the PVT electric system; 0,1,2 – initial stationary mode, external, internal nature of impacts.

The mathematical substantiation of maintenance of the operation of the PVT electric system Smart Grid (2), (Figure **1**), based on the methodology of the mathematical description of dynamics of power systems, the method of the graph of cause-effect relations [11] is proposed. The basis of the proposed rationale is the mathematical description of the architecture of the PVT electric system Smart Grid (1), (Figure **1**).

Where *PVTESSG* (τ) – operational maintenance of the Smart Grid PVT electric system; τ – time, seconds; *ID*(τ) – integrated dynamic subsystem (mains, photovoltaic solar panels, hybrid solar collectors, grid inverter, heat pump, two-section storage tank for, upper section for hot water supply, lower section as a low-grade energy source for heat pump, frequency converter). *P*(τ) – the properties of the elements of the integrated dynamic subsystem, units of the PVT electric system; *CMM*(τ,*z*) – complex mathematical modelling of the dynamics of changes in power factor, the local water temperature; *sd*(τ) – the input data (the solar electric system network with a capacity of 10 kW includes the following components: photovoltaic solar panels; hybrid solar panels ATMOSFERA-F2PV (Ukraine). The heat pump system – Commotherm Hybrid Tower WW, Split DeLuxe (Austria) with a heating capacity of 5.7 kW is equipped with a two-section storage tank, the lower section of which has a volume of 200 litres, used as a low-potential energy source connected to hybrid solar collectors. The upper section of it has a volume of 300 litres, used as a heat accumulator connected to hybrid solar collectors; *lp*(τ) – the boundary change in parameters (voltage from hybrid solar collectors at the grid inverter input, voltage at the frequency converter output and current frequency; *lf*(τ) – the levels of operation of the PVT electric system; *fd*(τ) – the obtained parameters (mode parameters of the PVT electric system); *tf*(τ,*z*) – the transfer function of predicted parameters: in the power factor, local water temperature; *AI*(τ,*z*) – reference information for assessing changes in power factor, the local water temperature; *C*(τ) – the control of operability of the PVT electric system; *LC*(τ) – the

logical relations of the operability control of the PVT electric system; *x*(τ) – impacts (change in solar radiation, change in consumption of electrical energy and heat; *f*(τ) – the measured parameters: (voltage at the grid inverter input from hybrid solar collectors, voltage at the frequency converter output, current frequencies); *K*(τ) – coefficients of mathematical description of the dynamics of power factor of the PVT electric system, the local water temperature;; *y*(τ, *z*) – predicted output parameters (power factor, the local water temperature); *z* – spatial coordinate of the condenser axis, heat exchanger coincides with the direction of the medium flow, metres; *d*(τ) – dynamic parameters of power factor change, the local water temperature change; *FI*(τ) – functional resulting information on decision-making; *LMD*(τ) – the logical relations of decision-making; *MD*(τ) – decision-making; *NC*(τ) – the new conditions of the PVT electric system; *S*(τ) – the identification of the state of the PVT electric system; *LS*(τ) – the logical relations of identification of the state of the PVT PVT electric system; *R*(τ) – the logical relations between the dynamic subsystem and units for charging, discharging, and functional estimation of efficiency that belong to the solar PVT electric system. Indices: *i* – the number of elements of *PVTESSG*(τ); 0,1,2 – the initial, external, and internal character of influences.

The mathematical substantiation of the architecture of the PVT electric system Smart Grid (1) and mathematical substantiation of maintenance of the operation of the PVT electric system Smart Grid (2) enable maintaining the operation of the PVT electric system using the following actions:

- operability control (*C*(τ)) of the dynamic subsystem based on complex mathematical (*CMM*(τ,*z*)) and logical (*LC*(τ)) modelling regarding obtaining standard (*AI*(τ,*z*)) estimate of a change in the power factor of a change in the local water temperature;
- operability control (*C*(τ)) of the dynamic system based on complex mathematical (*CMM*(τ,*z*)) and logical (*LC*(τ)) modelling regarding the obtaining functional (*FI*(τ)) estimate of a change in the power factor of the PVT electric system of a change in the local water temperature;
- decision-making (*MD*(τ)) with the use of the functional resulting information (*FI*(τ)), obtained based on logical modelling (*LMD*(τ)) to maintain the local water temperature by changing the power of the electric motor of the the compressor pump and circulation pump based on establishing the ratio of the voltage from hybrid solar collectors at the grid inverter input and the voltage at the frequency converter output are measured;
- identification (*S*(τ)) of the new operational conditions of the PVT electric system (*NC*(τ)) based on logical modelling (*LS*(τ)) as a part of the dynamic subsystem and confirmation of new operating conditions based on logical modelling (*R*(τ)) from the units of the PVT electric system.

3. COMPLEX MATHEMATICAL MODELLING OF HEAT PUMP POWER SUPPLY AND HOT WATER SUPPLY

According to formulas (1) and (2), the prediction of a change in the power factor of the PVT electric system and the local water temperature was proposed. The voltage at the inlet to the grid inverter from hybrid solar collectors, and the outlet from the frequency converter and current frequency are measured. The transfer function for the “power factor of the PVT electric system – voltage at the inlet to the grid inverter” relation is complex. A change in power factor and the local water temperature are estimated. A change in the local water temperature is estimated both over time and along the spatial coordinate of the condenser axis, heat exchanger coincides with the direction of the flow of motion of the medium. The transfer function for the “power factor of the PVT electric system – voltage at the inlet to the grid inverter” relation, which was obtained as a result of solving a system of nonlinear differential equations, is as follows:

$$W_{PF-U_1} = \frac{K_{\text{pf}} K_{\text{t}} \varepsilon \left(1 - L_{\text{e}}^*\right)}{\left(T_{\text{w}} S + 1\right)\beta - 1} \left(1 - e^{-\gamma \xi}\right), \tag{3}$$

where

$$K_{\text{pf}} = \frac{I(U_1 - U_2)}{(N_e)}; \quad K_{\text{t}} = \frac{m\left(\theta_{\text{o}} - \sigma_0\right)}{G_{i0}}; \quad \varepsilon = \frac{\alpha_{\text{e}0} h_{\text{e}0}}{\alpha_{\text{i}0} h_{\text{i}0}}; \quad L_{\text{e}}^* = \frac{1}{L_{\text{e}} + 1};$$

$$L_{\text{e}} = \frac{G_{\text{e}} C_{\text{e}}}{\alpha_{\text{e}0} h_{\text{e}0}}; \quad T_{\text{w}} = \frac{g_{\text{w}} C_{\text{w}}}{\alpha_{\text{i}0} h_{\text{i}0}}; \quad \beta = T_{\text{m}} S + \varepsilon^* + 1;$$

$$\varepsilon^* = \varepsilon(1 - L_{\text{e}}^*); \quad \gamma = \frac{(T_w S + 1)\beta - 1}{\beta}; \quad \xi = \frac{z}{L_{\text{i}}}; \quad L_{\text{i}} = \frac{G_{\text{i}} C_{\text{i}}}{\alpha_{\text{i}0} h_{\text{i}0}}.$$

where *PF* is the power factor of the PVT electric system; *I* – current, A; U_1 and U_2 – voltage at the grid inverter input and at the frequency converter output, respectively, volts; *Ne* – the power of the PVT electric system, kW; *C* is the specific thermal capacity, kJ/(kg·K); α is the heat transfer factor, kW/(m^2·K); *G* is the loss of substance, kg/s; *g* is the specific weight of a substance, kg/m; *h* is the specific surface, m^2/m; σ, θ are the temperature of the warming heat carrier and of the separating wall, respectively, K; *z* is spatial coordinate along the condenser axis, heat exchanger

coincides with the direction of the medium flow, metres; T_w and T_m are the time constants that characterize the thermal accumulation in local water and metal, seconds; m is the indicator of the dependence of heat transfer factor on consumption; τ is the time, seconds; S is the Laplace parameter, $S = \omega j$; ω is the frequency, 1/s. Indices: 0 – initial stationary mode; *i* – internal flow – local water; e – external flow – warming heat carrier; *m* – metal wall.

A real part of the transfer function was separated:

$$O(\omega) = \frac{(L_1 A_1) + (M_1 B_1) K_{pf} K_t \varepsilon (1 - L_e^*)}{(A_1^2 + B_1^2)}. \quad (4)$$

The K_t factor includes the temperature of the separating wall θ:

$$\theta = \left(\alpha_i \frac{(\sigma_1 + \sigma_2)}{2} + A \frac{(t_1 + t_2)}{2} \right) / (\alpha_i + A), \quad (5)$$

where σ_1 and σ_2 are the temperatures of the warming heat carrier at the inlet and the outlet of the heat exchanger, K, respectively; t_1 and t_2 are the local water temperatures at the heat exchanger inlet and outlet, K, respectively; α is the heat transfer factor, kW/(m^2·K). Index: *i* – local water.

$$A = \frac{1}{(\delta_m / \lambda_m + 1/\alpha_e)}, \quad (6)$$

where δ is the thickness of a wall of the heat exchanger, metres; λ is the thermal conductivity of the metal wall of the heat exchanger, kW/(m·K). Indices: e – warming heat carrier; *m* – metal wall of a heat exchanger. To use the real part $O(\omega)$, the following factors were obtained:

$$A_1 = \varepsilon^* - T_w T_m \omega^2; \quad (7)$$

$$A_2 = \varepsilon^* + 1; \quad (8)$$

$$B_1 = T_w \varepsilon \omega + T_w \omega + T_m \omega; \quad (9)$$

$$B_2 = T_m \omega; \quad (10)$$

$$C_1 = \frac{A_1 A_2 + B_1 B_2}{A_2^2 + B_2^2}; \quad (11)$$

$$D_1 = \frac{A_2 B_1 - A_1 B_2}{A_2^2 + B_2^2}; \quad (12)$$

$$L_1 = 1 - e^{-\xi C_1} \cos(-\xi D_1); \quad (13)$$

$$M_1 = -e^{-\xi C_1} \sin(-\xi D_1). \quad (14)$$

The transfer function (3), which was obtained based on the use of the operator method of solving the system of nonlinear differential equations, retains the Laplace transform parameter – S(S=ωj), where ω is the frequency, 1/s. To switch from the frequency area to the time area, a real part (4), obtained as a result of the mathematical treatment of the transfer function, was separated. It is this part that is included in the integrals (15) and (16), which makes it possible to obtain dynamic characteristics of a change in power factor of the PVT electric electric, the local water temperature using the inverse Fourier transform:

$$PF(\tau) = \frac{1}{2\pi} \int_0^\infty K_{pf} K_t O(\omega) \sin(\tau\omega/\omega) d\omega, \quad (15)$$

$$t(\tau, z) = \frac{1}{2\pi} \int_0^\infty K_{pf} K_t O(\omega) \sin(\tau\omega/\omega) d\omega, \quad (16)$$

where *PF* is the power factor of the PVT electric system; *t* is the local water temperature, K.

Analyzing the mathematical model, we set the internal parameters included in the coefficients of the dynamics equations. Under real power system operating conditions, during transitions from steady-state modes and the impact of external and internal factors such as changes in solar radiation and electrical and thermal energy consumption, the coefficients of the K_t and K_{pf} dynamics equations are adjusted over time depending on changes in internal diagnostic parameters: the voltage of the grid inverter from hybrid solar collectors, and the output voltage of the frequency converter. The coefficients of the K_t and K_{pf} dynamics equations change over time depending on changes in the measured ratio of the input voltage of the grid inverter from the hybrid solar collectors to the output voltage of the frequency converter.

The PVT electric system network with a capacity of 10 kW includes the following components: photovoltaic solar panels; hybrid solar panels ATMOSFERA-F2PV (Ukraine). The heat pump system – Commotherm Hybrid Tower WW, Split DeLuxe (Austria) with a heating capacity of 5.7 kW is equipped with a two-section storage tank, the lower section of which has a volume of 200 litres, used as a low-potential energy source connected to hybrid solar collectors. The upper section of it has a volume of 300 litres, used as a heat accumulator connected to hybrid solar collectors for hot water supply.

The following levels of operation of the heat pump system have been established for the change in the temperature of the refrigerant at the inlet to the condenser and at the outlet from the condenser: first level – 45–40.5°C; second level – 50–45.5°C; third level – 55–50.5°C; fourth level – 60–55.5°C. They correspond to changes in the local water temperature: 35–40°C; 40–45°C; 45–50°C; 50–55°C. The temperature of the low-potential energy source –

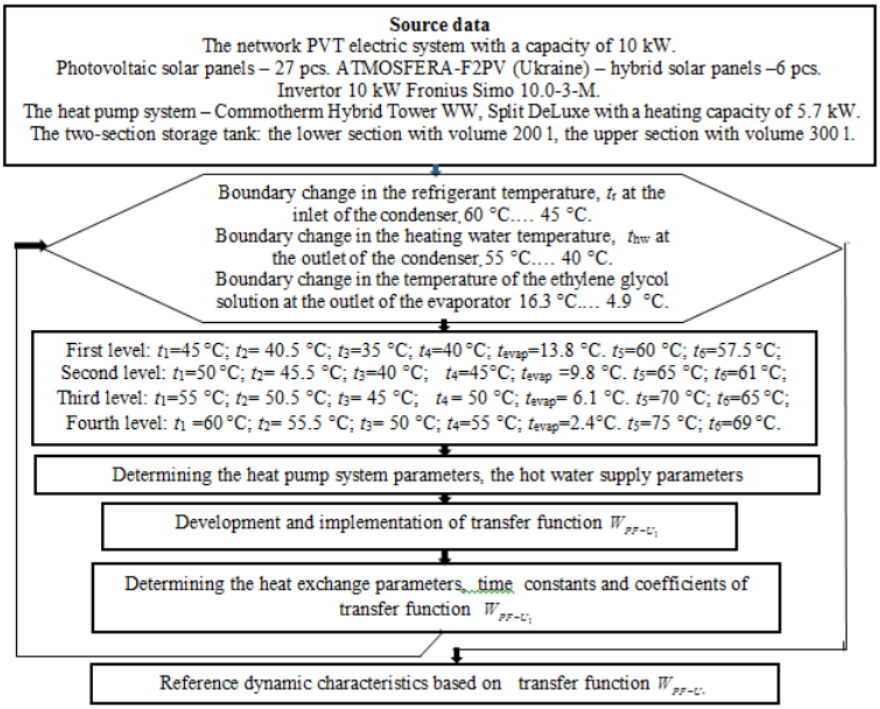

Figure 2: Block diagram of comprehensive mathematical modelling of the PVT electric system: t_1 and t_2 – the refrigerant temperature at the inlet of the condenser and the outlet of the condenser, respectively, °C; t_3 and t_4 – the local water temperature at the inlet of the condenser and the outlet of the condenser, respectively, °C; t_5 and t_6 – the temperature of the water from hybrid solar collectors at the inlet to the heat accumulator and at the outlet from the heat accumulator for hot water supply, respectively, °C; t_{evap} – the refrigerant evaporation temperature.

ethylene glycol solution at the outlet of the heat pump evaporator is: 16.3°C, 12.3°C, 8.6°C, 4.9°C, corresponding to the established operating levels for heating up to a temperature of 20°C. The following levels of operation of the hot water supply have been established for the change in the temperature of the water from hybrid solar collectors at the inlet to the heat accumulator and at the outlet from the heat accumulator: first level: 60–57.5°C; second level: 65–61°C; third level: 70–65°C; fourth level: 75–69°C. They correspond to changes in the local water temperature: 30–55°C. Warming heat carrier consumption – 0.095 kg/s.

According to formulas (1)–(3), the results of complex mathematical modelling of the heat pump power supply and hot water supply using hybrid solar collectors are presented (Figure **2**, Tables **1**–**6**).

Table 1: Operating Parameters of the Heat Pump System

Levels of operation	G_r, kg/s	N_e, kW	N_t, kW	*U*, V	*f*, Hz	*n*, rpm	*COP*
first level	0.0340	0.705	1.4	194.2	24.28	738.4	8.08
second level	0.0350	0.923	2.9	254.3	31.78	953.4	6.17
third level	0.0357	1.185	4.3	326.5	40.81	1224.3	4.80
fourth level	0.0363	1.452	5.7	400	50	1500	3.92

Note: G_r – refrigerant consumption, kg/s; N_e – power of the compressor electric motor, kW; N_t – thermal power of the low-grade energy source, kW; *U* – voltage, volts; *f* – current frequency, Hz; *n* – the number of revolutions of the compressor electric motor, rpm; *COP* – coefficient of performance of the heat pump system.

Table 2: Operating Parameters of the Hot Water Supply

Levels of operation	G_w, kg/s	N_t, kW	*U*, V	*f*, Hz	*n*, rpm
first level	0.0090	1	92	20	1140
second level	0.0100	1.5	138	30	1710
third level	0.0106	2	184	40	2280
fourth level	0.0120	2.5	230	50	2850

Note: G_w – local water consumption, kg/s; N_t – heating power, kW; *U* – voltage, volts; *f* – voltage frequency, Hz; *n* – the number of revolutions of the circulation pump electric motor, rpm.

Table 3: Heat Transfer Parameters as Part of Complex Mathematical Modelling of Heat Pump Power Supply

Levels of operation	Parameters		
	α_r, kW /(m^2·K)	α_w, kW /(m^2·K)	*k*, kW /(m^2·K)
first level	1.15	0.785	0.460
second level	1.19	0.901	0.505
third level	1.26	1.076	0.570
fourth level	1.38	1.372	0.674

Note: α_r – coefficient of convective heat transfer from the refrigerant to the condenser wall, kW /(m^2·K); α_w – coefficient of convective heat transfer from the condenser wall to local water, kW /(m^2·K); *k* – heat transfer coefficient, kW /(m^2·K).

Table 4: Heat Transfer Parameters as Part of Complex Mathematical Modelling of the Hot Water Supply

Levels of Operation	Parameters		
	α_e, kW /(m^2·K)	α_w, kW /(m^2·K)	*k*, kW /(m^2·K)
first level	1.513	0.749	0.486
second level	1.533	0.851	0.530
third level	1.549	0.927	0.560
fourth level	1.555	0.953	0.564

Note: α_e– coefficient of convective heat transfer from the warming heat carrier to the heat exchanger wall, kW /(m^2·K); α_w – coefficient of convective heat transfer from the heat exchanger wall to local water, kW /(m^2·K); *k* – heat transfer coefficient, kW /(m$_2$·K).

The time constants and coefficients of the mathematical model of the dynamics of change in the efficiency coefficient and temperature of the heated water for heat pump power supply (Table **5**) are determined on the basis of the data presented in the Tables **1**,**3**.

The time constants and coefficients of the mathematical model of the dynamics of change in the efficiency coefficient and temperature of the heated water for the hot water power supply (Table **6**) are determined on the basis of the data presented in the Tables **2**,**4**.

Based on the proposed mathematical substantiation Smart Grid maintenance of functioning of the PVT electric system (1) to (3) the block diagram for the control of serviceability of the PVT electric system (Figure **3**) is developed.

Table 5: Time Constants and Coefficients of the Mathematical Model of the Dynamics of the Temperature of the Water of the Heat Pump Power Supply

Levels of Operation	T_w, s	T_m, s	L_w, m	ε	L_e, m	L_e^*	ε*	ζ
first level	6.23	2.62	24.61	1.7756	2.50	0.2857	1.2683	0.6811
second level	5.42	2.28	21.43	1.6014	2.48	0.2874	1.1412	0.6309
third level	4.54	1.91	17.95	1.4182	2.44	0.2907	1.0059	0.5945
fourth level	3.56	1.50	14.08	1.2204	2.30	0.3030	0.8506	0.5794

Note: T_w and T_m – time constants characterizing the local water thermal storage capacity, metal, seconds; L_w, L_e, L_e*, ε, ε*, ζ – coefficients of the mathematical model of the local water temperature dynamics.

Table 6: Time Constants and Coefficients of the Mathematical Model of the Dynamics of the Temperature of the Water of the Hot Water Power Supply

Levels of operation	T_w, s	T_m, s	L_w, m	ε	L_e, м	L_e *	ε*	ζ
First level	37.4	7.96	0.59	1.72	3.65	0.22	1.34	2.8
Second level	32.9	7.0	0.58	1.53	3.61	0.22	1.19	2.85
Third level	30.2	6.43	0.56	1.42	3.57	0.22	1.11	2.95
Fourth level	29.4	6.26	0.62	1.39	3.55	0.22	1.08	2.66

Note: T_w, T_m – time constants characterizing the local water thermal storage capacity, metal, seconds; L_w, L_e, L_e*, ε, ε*, ζ – coefficients of the mathematical model of the local water temperature dynamics.

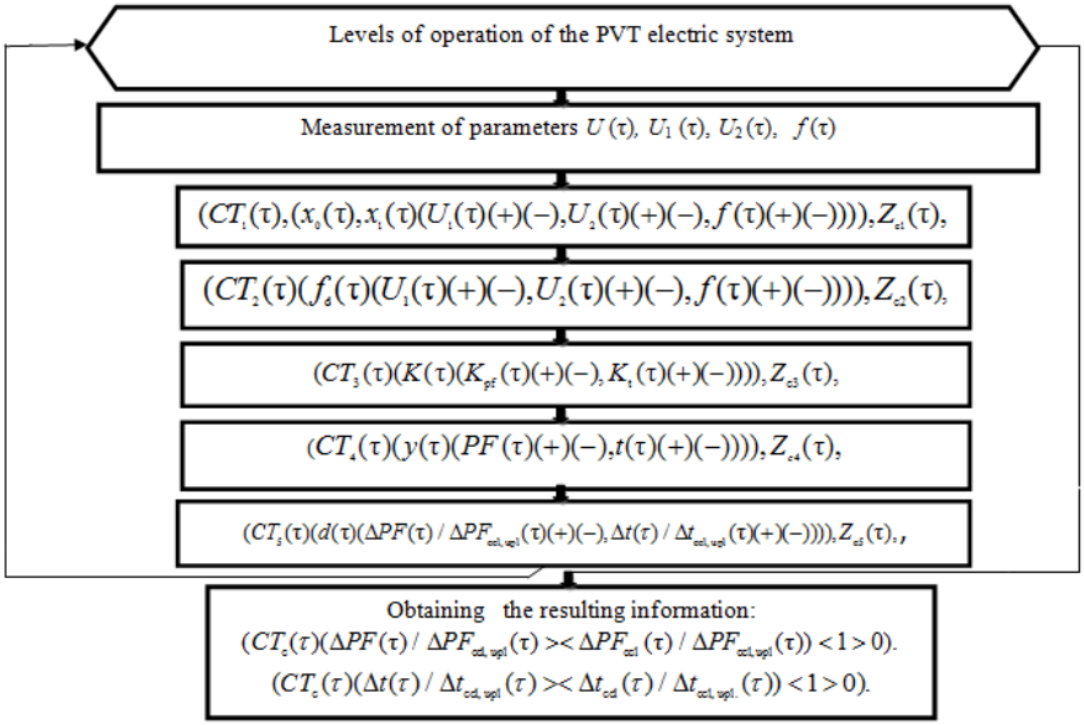

Figure 3: Block diagram of the PVT electric system operational control: *U, U*$_1$, *U*$_2$ – voltage at the network inverter input, voltage at the network inverter input from hybrid solar collectors and the frequency converter output; *f* – current frequency, Hz; *PF* – power factor of the PVT electric system; *t* – local water temperature, °C; *CT* – event control; *Z* – logical relations; *d* – dynamic parameters; *x* – effects; f_d – parameters measured; *y* – parameters predicted; *K* – coefficients of mathematical description; ι – time. Indices: *c* – control of operability; ccl upl – the constant calculated value of the parameter of the lower and upper levels of operation (heat pump power supply), (hot water power supply), respectively; ccl – the constant calculated value of the operation level parameter; 0,1,2 – initial stationary mode, external, internal influences; 3 – coefficients of dynamics equations; 4 – significant predicted parameters; 5 – dynamic parameters.

Control of operability of the PVT electric system (Figure **3**) enables obtaining the resulting information for on advance decision-making about the harmonization of production and consumption of PVT electric system. Based on the proposed mathematical substantiation Smart Grid (1) to (3) the block diagram of maintenance of operation of the PVT electric system (Figure **4**) is developed.

Maintaining the transmission of electrical energy to the grid allows the production and consumption of electrical energy to be coordinated (Figure **4**).

4. RESULTS AND DISCUSSION

4.1. Smart Grid PVT Electric System at the Decision-Making Level

Harmonization of electric power production and consumption in the heat pump power supply

A comprehensive integrated support system for a PVT electric system has been developed based on the power supply system of a heat pump, whose low-potential energy source, acting as a storage tank, is connected to hybrid solar collectors (Table **7**, Figure **5**).

The system is based on the predicted power factor of the PVT electric system and local water temperature changes. The voltage at the input of the grid-tie inverter from the hybrid solar collectors, the output voltage of the frequency converter, and the current frequency are continuously measured. Proactive decisions are made to adjust the power of the heat pump compressor motor in accordance with changes in the thermal output of the lower section of the two-section storage tank, which serves as a low-potential energy source. The power factor of the PVT electric system over a given period is determined as follows:

$$PF_{i+1}(\tau) = PF_i + \\ + \begin{pmatrix} \Delta PF_{i+1}(\tau)/\Delta PF_{1..}(\tau) - \\ -\Delta PF_i(\tau)/\Delta PF_1(\tau) \end{pmatrix} (PF_2 - PF_1), \quad (17)$$

where *PF* is the power factor of the PVT electric system; PF_1 and PF_2 are the initial, final values of power factor; τ is the time, seconds. Index: 1 is the constant, calculated value of the parameter of the lower operational level; *i* is the number of levels of the PVT electric system operation.

The local water temperature in the established period is determined as follows:

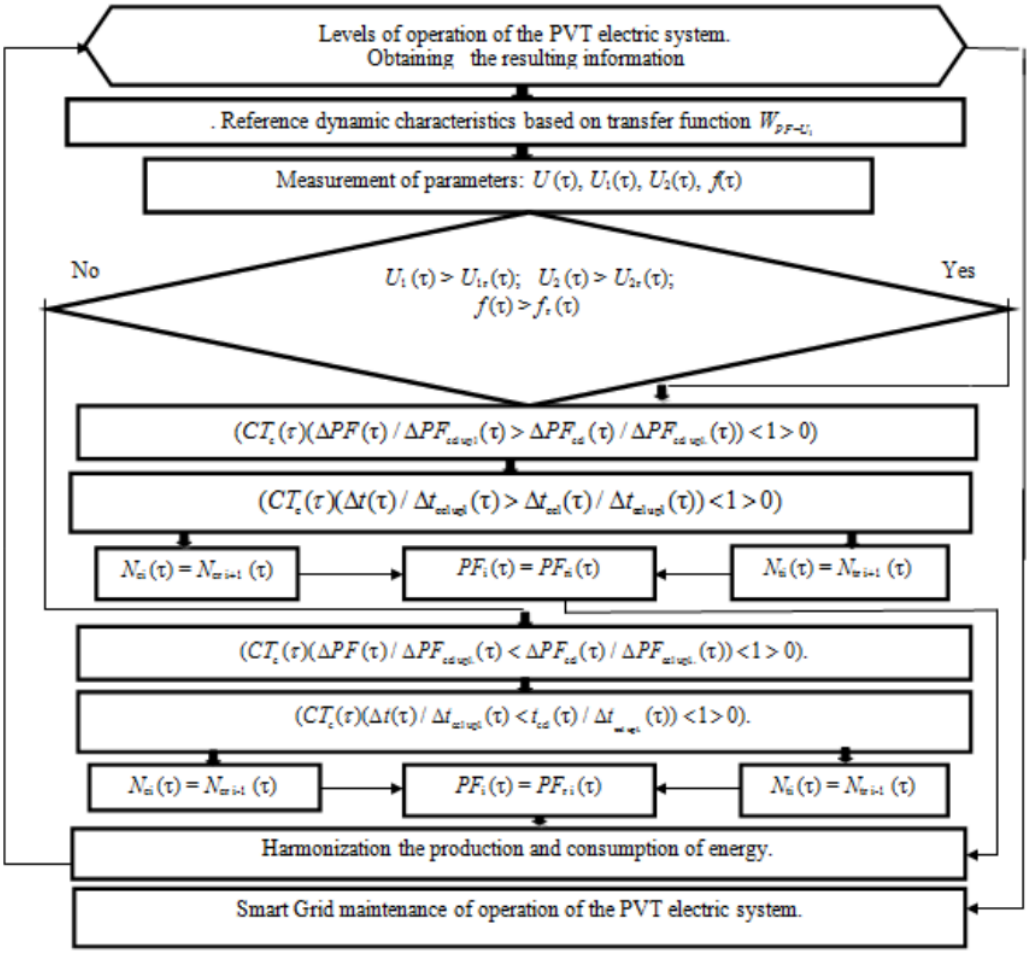

Figure 4: Block diagram of operational maintenance of the PVT electric system: *U, U*$_1$, *U*$_2$ – voltage at the network inverter input, voltage at the network inverter input from hybrid solar collectors and the frequency converter output; *f* – current frequency, Hz; *PF* – power factor of the PVT electric system; N_e, N_t – power of the compressor electric motor, heating power, respectively, kW; ι – time; Indices: *i* – number of operation levels; r – reference value of the parameter; ccl upl – constant calculated value of the parameter of the lower and upper levels of operation (heat pump power supply), (hot water power supply), respectively; ccl – constant calculated value of the operation level parameter.

$$t_{wi+1}(\tau) = t_{wi} + \left(\left(\frac{\Delta t_{wi+1}(\tau)}{\Delta t_{1.}(\tau)} - \frac{\Delta t_{wi}(\tau)}{\Delta t_{1}(\tau)} \right) (t_{w2} - t_{w1}) \right), \quad (18)$$

where t_w – local water temperature, °C; t_1, t_2 – initial and final values of local water temperature, °C, respectively; *i* – the number of operational levels; τ – time, seconds. Index 1 – the constant, calculated value of the lower operational level parameter.

So, for example, in the period of time $147 \cdot 10^5$ s (4083 h) from the beginning of the heating season, the predicted increase in the power factor went from 0.8570 to 0.8586. The power factor using formula (17) is:

0.8586 = 0.8570 + (0.3125-0.3080)(0.98-0.95)

In the period of time $147 \cdot 10^5$ s (4083 h), the predicted increase in the local water temperature went from 48.92°C to 49°C. The local water temperature using formula (18) is:

49°C = 48.92°C+(0.3125–0.3080)(55°C–35°C).

During this period, when the voltage at the grid inverter input from the hybrid solar collectors changes to 257.9 V, it is necessary to make a decision to maintain the solar electrical system's power factor at 0.8586. Predicting an increase in the thermal power of the lower section of the two-section storage tank as a low-potential energy source for the heat pump, it is necessary to increase the power of the heat pump compressor electric motor based on the current frequency change to 40.81 Hz. Also, it is necessary to increase the power level of the grid-connected power supply from 0.8. Adopting a proactive decision to increase the number of revolutions of the compressor electric motor enables increasing the refrigerant consumption to the level of 0.0357 kg/s and ensuring the maintenance of the local water temperature at 49°C. The implementation of such actions will enable coordinating the production and consumption of energy

Table 7: Integrated Smart Grid System for Harmonization of Electric Power Production and Consumption in the Heat Pump Power Supply

Time, τ, 10^3 s	Changing the parameters	ΔPF(τ) /ΔPF$_1$(τ)	PF(τ)	t_w(τ), °C
0	Charging.U = 200V; U_1 = 84 V; U_2 = 190.7 V; f = 25.09 Hz; G_r = 0.0340 kg/s; $t_{r\,in}$ = 45°C; t_{rout} = 40.5°C; $t_{w\,in}$ = 35°C; $t_{w\,out.}$ = 40°C; m = 0.33	1	0.58	35
10.5	Charging.U = 220V; U_1 = 90 V U_2 = 190.7 V;$t_{r\,in}$ = 45°C; ; t_{rout} = 0.5°C; $t_{w\,in}$ = 35°C; $t_{w\,out.}$ = 40°C; m = 0.37	0.9438	0.6025	36.12
21	Charging.U = 240V; U_1 = 96 V; U_2 = 190.7 V; $t_{r\,in}$ = 45°C;t_{rout} = 40.5°C; $t_{w\,in}$ = 35°C; $t_{w\,out}$ = 40°C; m = 0.4	0.8875	0.6250	37.25
31.5	Charging.U = 260V; U_1 = 108 V; U_2 = 190.7 V; $t_{r\,in}$ = 45°C; t_{rout} = 40.5°C; $t_{w\,in}$ = 35°C; $t_{w\,out}$ = 40°C; m = 0.43	0.7751	0.6700	39.5
42	Charging.U = 280V; U_1 =114 V; U_2 = 190.7 V; $t_{r\,in}$ = 45°C; t_{rout} = 40.5°C; $t_{w\,in}$ = 35°C; $t_{w\,out}$ = 40°C; m = 0.47	0.7188	0.6925	40.63
52.5	Charging.U = 300V; U_1 = 126 V; U_2 = 190.7 V; $t_{r\,in}$ = 45°C;t_{rout} = 40.5°C; $t_{w\,in}$ = 35°C; $t_{w\,out}$ = 40°C; m = 0.5	0.6064	0.7375	42.88
63	Charging.U = 320V; U_1 = 130 V; U_2 = 190.7 V; $t_{r\,in}$ = 45°C;t_{rout} = 40.5°C; $t_{w\,in}$ = 35°C; $t_{w\,out.}$ = 40°C; m = 0.53	0.5689	0.7525	43.63
73.5	Charging.U = 340V; U_1 = 136 V; U_2 = 190.7 V; $t_{r\,in}$ = 45°C;t_{rout} = 40.5°C; $t_{w\,in}$ = 35°C; $t_{w\,out}$ = 40°C; m = 0.57	0.5126	0.7750	44.76
84	Charging.U = 360V; U_1 = 140 V; U_2 = 190,7 V; $t_{r\,in}$ = 45°C;t_{rout} = 40.5°C; $t_{w\,in}$ = 35°C; $t_{w\,out}$ = 40°C; m = 0.60	0.4752	0.7900	45.51
94.5	Decision on discharging.U = 380V; Gr = 0.035 kg/s; U_1 = 173.96 V; U_2= 241.56 V; f = 31.78 Hz; $t_{r\,in}$ = 50°C; $t_{rout.}$ = 45.5°C $t_{w\,in}$ = 40°C; $t_{w\,out.}$ = 45°C; m = 0.63	0.4783	0.7912	45.51
105	Charging.U = 400V; U_1 = 179.96 V; U_2 = 241.56 V; f = 31.78 Hz;$t_{r\,in}$ = 50°C; $t_{rout.}$ = 45.5°C; $t_{w\,in}$ = 40°C; $t_{w\,out.}$ = 45°C; m = 0.67	0.4355	0.8083	46.37
115.5	Charging.U = 420V; U_1 = 185.96 V; U_2 = 241.56 V; $t_{r\,in}$ = 50°C; $t_{rout.}$ = 45,5°C; $t_{w\,in}$ = 40°C; $t_{w\,out.}$ = 45°C; m = 0.7	0.3931	0.8253	47.22
126	U = 440V; U_1 = 191.96 V; U_2 = 241.56 V; $t_{r\,in}$ = 50°C; $t_{rout.}$ = 45.5°C; $t_{w\,in}$ = 40°C; $t_{w\,out.}$ = 45°C; m = 0.73	0.3506	0.84	48.07
136.5	Charging.U = 460V; U_1 = 197.96 V; U_2 = 241.56 V; $t_{r\,in}$ = 50°C; $t_{r\,out.}$ = 45,5°C; $t_{w\,in}$ = 40°C; $t_{w\,out.}$ = 45°C; m = 0.77	0.3082	0.8570	48.92
147	Decision on discharging. U = 480V; U_1 = 257.9 V; U_2 = 310.17 V; G_r = 0.0357 kg/s; f = 40.81 Hz; $t_{r\,in}$ = 55°C; ; $t_{rout.}$ = 50.5°C; $t_{w\,in}$ = 45°C; $t_{w\,out.}$ = 50°C; m = 0.8	0.3125	0.8586	49
157.5	Charging.U = 500V; U_1 = 281.9 V; U_2 = 310.17 V; f = 40.81 Hz; $t_{r\,in}$ = 55°C; $t_{rout.}$ = 50.5°C; $t_{w\,in}$ $t_{w\,in}$ = 45°C; $t_{w\,out.}$ = 50°C; m = 0.83	0.1690	0.9154	51.87
161.6	Decision on discharging. U = 540V; U_1 = 341.93 V; U_2 = 380V;Gr = 0.0363 kg/s; f = 50 Hz; $t_{r\,in}$ = 60°C; ; $t_{rout.}$ = 55.5°C; $t_{w\,in}$ = 50°C; $t_{w\,out.}$ = 55°C; m = 0.9	0.0690	0.9554	53.67
161.6	Discharging.U = 600V; U_1 = 341.93 V; U_2 = 380 V; f = 50 Hz; G_r = 0.0363 kg/s; $t_{r\,in}$ = 60°C; ; $t_{rout.}$ = 55.5°C; $t_{w\,in}$ = 50°C; $t_{w\,out.}$ = 55°C; m = 1	0	0.98	55

Note: PF – power factor; $t_{r\,in}$, t_{rout}, $t_{w\,in}$, $t_{w\,out}$ – refrigerant temperature, local water temperature at the inlet to the condenser, at the outlet from the condenser, °C; G_r – refrigerant consumption, kg/s; f – current frequency, Hz; U, U_1 U_2 – voltage at the network inverter input, voltage at the network inverter input from hybrid solar collectors and the frequency converter output, volts; m – level of transmission of electricity to the network; τ – time, seconds. Indices: w – internal flow – local water; 1 – constant, calculated value of the parameter of the lower operational level

while maintaining the operation of the heat pump power supply.

Harmonization of electric power production and consumption in the hot water power supply

A complex integrated system for supporting the operation of the hot water power supply has been developed (Table **8**, Figure **6**).

This system is based on the predicted power factor and local water temperature changes. The voltage at the grid inverter from hybrid solar collectors input, the

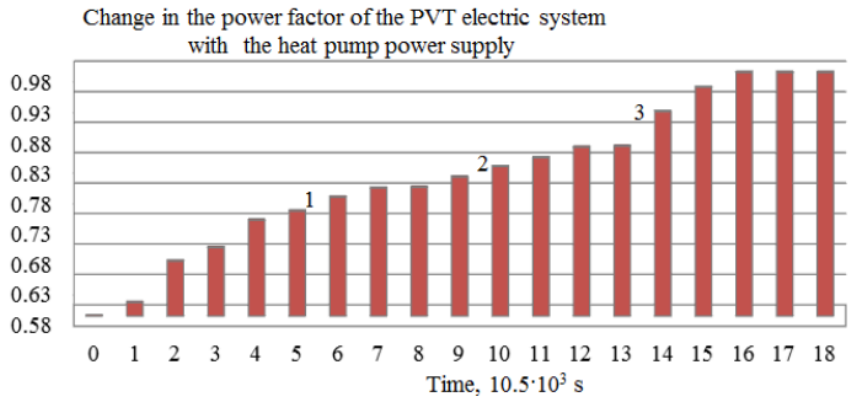

Figure 5: Operational maintenance of the PVT electric system. 1, 2, and 3 are the points when decisions were made on changing the power level in the electric motor of the heat pump compressor in accordance with the change in the thermal power of the lower section of the two-section storage tank as a low-potential energy source.

Table 8: Integrated Smart Grid System for Harmonization of Electric Power Production and Consumption in the Hot Water Power Supply

Time, τ, 10^3 s	Changing the parameters	ΔPF(τ) /ΔPF$_1$(τ)	PF(τ)	t_w(τ), °C
3	Charging. U = 240V; N_e = 4 kW; U_1 = 32 V; U_2 = 38.8 V; f = 8.43 Hz; G_w = 0.009 kg/s; t_{in} = 60°C; t_{out} = 57.5°C; m = 0.4	0.1435	0.6374	33.59
6	Charging. U = 280V; N_e = 4.7 kW; U_1 = 72 V; U_2 = 86.27 V; f = 18.75 Hz; G_w = 0.009 kg/s; t_{in} = 60°C; t_{out} = 57.5°C; m = 0.47	0.3010	0.7004	37.53
9	Decision on discharging. U = 320V; N_e = 5.3 kW; G_w = 0.0100 kg/s; U_1 = 72 V; U_2 = 86.27 V; f = 18.75 Hz; t_{in} = 65°C; t_{out} = 61°C; m = 0.53	0.3256	0.7102	38.14
12	Charging. U = 360V; N_e = 6 kW;U_1 = 108 V; U_2 = 129.4 V; f = 28.13 Hz; G_w = 0.010 kg/s; t_{in} = 65°C; t_{out} = 61°C; m = 0.60	0.4883	0.7753	42.21
15	Decision on discharging. U = 400V; N_e = 6.7 kW; G_w = 0.0106 kg/s; U_1 = 108 V; U_2 = 129.4 V; f = 28.13 Hz; t_{in} = 70°C; t_{out} = 65°C; m = 0.67	0.5567	0.8027	43.92
18	Charging.U = 440V; N_e = 7.3 kW; U_1 = 144 V; U_2 = 172.5 V; f = 37.5 Hz; G_w = 0.0106 kg/s; t_{in} = 70°C; t_{out} = 65°C; m = 0.73	0.7415	0.8766	48.54
21	Charging.U = 480V; N_e = 8 kW; U_1 = 180 V; U_2 = 215.7 V; f = 46.9 Hz; G_w = 0.0106 kg/s; t_{in} = 70°C; t_{out} = 65°C; m = 0.80	0.9288	0.9515	53.22
24	Decision on discharging.U = 520V; N_e = 8.7 kW; G_w = 0.0120 kg/s; U_1 = 180 V; U_2 = 215.7 V; f = 46.9 Hz; t_{in} = 75°C; t_{out} = 69°C; m = 0.87	0.9395	0.9558	53.49
27	Discharging.U = 560V; N_e = 9.3 kW;U_1 = 182 B; U_2 = 230 B; f = 50 Hz; G_w = 0.0120 kg/s; t_{in} = 75°C; t_{out} = 69°C; m = 0.93		0.98	55
30	Discharging.U = 600V; Ne = 10 kW; U_1 = 182 B; U_2 = 230 B; f = 50 Hz; G_w = 0.0120 kg/s; t_{in} = 75°C; t_{out} = 69°C; m = 1	1	0.98	55

Note: PF – power factor; tin, tout – warming heat carrier temperature at the inlet to the heat exchanger, at the outlet from the heat exchanger, °C; t_w – local water temperature, °C; G_w – local water consumption, kg/s; f – current frequency, Hz; U, U_1 U_2 – voltage at the network inverter input, voltage at the network inverter input from hybrid solar collectors and the frequency converter output, volts; τ – time, seconds. Indices:w – local water; 1 – constant, calculated value of the parameter of the upper level.

voltage at the frequency converter output and the current frequency are continuously measured. Advance decisions are made to change the power of the electric motor of the circulation pump, based on the change in the current frequency in accordance with the change in the thermal power of the upper section of the two-section storage tank.

Thus, for example, in the period of time $15 \cdot 10^3$ s (4.2 h) from the beginning of the predicted increase power factor of the solar radiation from 0.7753 to 0.8027 the power factor using formula (17) is:

$$0.8027 = 0.7753 + (0.5567 - 0.4883)(0.98 - 0.95).$$

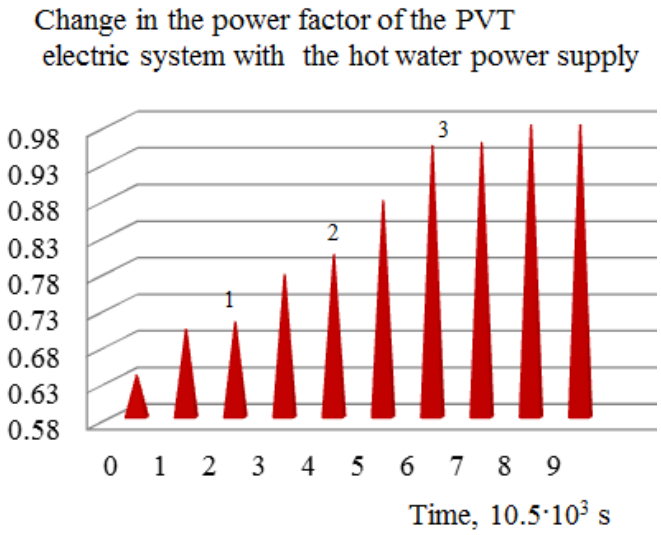

Figure 6: Operational maintenance of the PVT electric system. 1, 2, and 3 are the points when decisions were made on changing the power level in the electric motor of the circulation pump in accordance with the change in the thermal power of the upper section of the two-section storage tank.

In this period of time $15 \cdot 10^3$ s (4.2 h), the predicted increase in the local water temperature went from 42.21°C to 43.92°C. The local water temperature using formula (18) is:

$$43.92°C = 42.21°C + (0.5567-0.4883)(55°C–30°C).$$

During this period, when the voltage at the grid inverter input from the hybrid solar collectors changes to 108 V, it is necessary to make a decision to maintain the solar electrical system's power factor at 0.8027. Anticipating an increase in the thermal power of the upper section of the two-section solar storage tank, it is necessary to increase the power of the circulation pump's electric motor, based on a change in the current frequency to 28.13 Hz. Also, it is necessary to increase the power level of the grid-connected power supply from 0.6. Making a proactive decision to increase the electric motor speed allows increasing the local water flow to 0.0106 kg/s and maintaining the local water temperature at 43.92°C. Implementation of these measures will coordinate energy production and consumption, maintaining the operation of the hot water supply system.

5. CONCLUSIONS

1. Integrated Smart Grid system has been developed to harmonize electricity production and consumption in heat pump and hot water supply systems. Modern solutions have been implemented to adjust the power of the heat pump compressor motor and the circulation pump motor in response to changes in the thermal output of storage tanks connected to hybrid solar collectors. When the grid inverter input voltage changes from 200 V to 600 V, the power transmitted to the grid increases from 0.33 to 1, and the power factor increases by 40% while maintaining the temperature of the heated water at 35–55°C. Determining the final functional information allows for early decisions to be made about changing the operating mode of the heat pump compressor motor and the circulating motor to prevent peak loads on the power grid and maintain voltage in the distributed system.

2. The structural diagram has been developed and complex mathematical modeling of heat pump power supply and hot water supply has been applied to obtain a reference and functional estimates of the change in the power factor and hot water temperature of the grid-tied solar power system. Estimation of the measured ratio of voltages at the input of the grid-tied inverter from hybrid solar collectors and the output of the frequency converter is a unifying element of the mathematical modeling of the dynamics. The heat exchange parameters in the heat pump and hot water supply system, time constants and coefficients of the mathematical models of the dynamics for steady-state operating modes have been determined. Reference and functional dynamic estimates of the change in the power factor in the range of 0.58 – 0.98, and the temperature of heated water in the range of 35–55°C for heat pump power supply and in the range of 0.6374 – 0.98 and the temperature of 35–55°C for hot water supply in accordance with operational levels have been obtained.

3. The structural diagram of logical modeling of the integrated control of a grid-connected solar energy system based on the cause-and-effect principle has been developed. Based on the structural diagram, changes in voltage at the grid-connected inverter input, at the grid-connected inverter input from hybrid solar collectors, at the frequency converter output, current

frequency, coefficients of mathematical models of the dynamics of changes in the power factors and the temperature of heated water, K_t and K_{pf}, and dynamic parameters of changes in the coefficients of mathematical models of the power and temperature of heated water have been estimated. The resulting performance monitoring block allows for obtaining a resulting functional assessment of changes in the power factor and temperature of heated water for decision-making in real operating conditions under the influence of external and internal disturbances in the range of voltage changes at the grid-connected inverter input from 200 to 600 V. The coefficients of the mathematical equations of the K_t and K_{pf} dynamics change over time due to changes in the measured ratio of the input voltage of the grid-connected inverter from the hybrid solar collectors to the output voltage of the frequency converter.

4. The structural diagram was developed and logical modeling was conducted to obtain final information at the decision-making level regarding changes in the heat pump compressor motor power. Predictable solutions have been implemented for regulating the heat pump compressor motor power in response to changes in the thermal output of the lower section of the storage tank, which serves as a low-potential energy source connected to hybrid solar collectors. Thus, when the voltage at the grid-tie inverter input from the hybrid solar collectors changes from 84 to 341.93V, voltage at he frequency converter output from 190.7 to 380 V and the thermal output of the storage tank is predicted to increase from 1.4 to 5.7 kW, it is necessary to increase the power of the heat pump compressor motor from 0.705 to 1.452 kW. Making a proactive decision to increase the compressor motor speed allows for an increase in refrigerant flow rate from 0.0340 to 0.0363 kg/s and maintains the temperature of the heated water at 35–55°C. The power factor of the grid-tied solar power system is maintained in the range of 0.58–0.98 when the voltage at the grid-tied inverter input changes from 200 to 600 V, with the power transmission level to the grid ranging from 0.33 to 1.

5. The structural diagram and conduct logical modeling to obtain final information at the decision-making level for changing the power of the circulation pump.Predictable solutions have been implemented for regulating the power of the circulation pump motor to provide hot water supply in accordance with changes in the thermal output of the upper section of the storage tank connected to hybrid solar collectors. Thus, when the voltage at the grid-tie inverter input from the hybrid solar collectors changes from 32 to 182 V, voltage at he frequency converter output from 38.8 to 230 V and the thermal output of the storage tank is projected to increase from 1 to 2.5 kW, it is necessary to increase the power of the circulation pump motor from 1140 to 2850 rpm. Making a proactive decision to increase the speed of the circulation pump motor allows for an increase in the flow rate of heated water from 0.0900 to 0.0120 kg/s and maintains the temperature of the heated water at 35–55°C. The power factor of the grid-tied solar power system is maintained in the range of 0.6374–0.98 when the grid-tied inverter input voltage varies from 200 to 600 V, with the grid-tied power transmission level ranging from 0.4 to 1.

6. Coordination of electricity production and consumption was achieved by predicting changes in the power factor and temperature of the heated water. Advanced solutions for adjusting the power level of the heat pump and circulation pump, in coordination with the thermal capacity of the storage tanks, made it possible to adjust the level of electricity transmitted to the grid__When the grid-tie inverter input voltage changes from 200 V to 600 V, the power transmitted to the grid increases in the range of 0.33 to 1, the power factor by 40%. Determining the final functional information allows for early decisions to be made about changing the operating mode of the heat pump compressor motor and the circulating motor to prevent peak loads on the power grid and maintain voltage in the distributed system. Research in this area can be continued to improve control systems for connecting, for example, backup power supplies and new baseload renewable.

CONFLICTS OF INTEREST

The author declared no conflicts of interest.

REFERENCES

[1] Chaikovskaya E. Biogas Heat Pump Power Supply Based on Smart Grid Functioning Solar Electric System Network. Journal of Solar Energy Research Updates, 2024, 11,58-67. https://doi.org/10.31875/2410-2199.2024.11.07

[2] Chaikovskaya E. Smart Grid Functioning of Solar Electric System Network Based on Complex Accumulation Control. Journal of Solar Energy Research Updates, 2023, 10, 54- 65. https://doi.org/10.31875/2410-2199.2023.10.06

[3] Zhanhun Liang, Jinjian Xie, Jiayi Deng, Yan Jiang and Hai Wang. Design and Testing of Transmissive Fresnel Concentration and Thermoelectric Power Generation System. Journal of Solar Energy Research Updates, 2025, 12, 1- 5. https://doi.org/10.31875/2410-2199.2025.12.01

[4] Muhammad Umair Hassan, Muhammad Sumair Hassan and Bjarte Hoff.Using Point of Common Coupling (PCC) for Power Shaving in Grid Connected Hybridized Network. Journal of Solar Energy Research Updates, 2025, 12,6-29. https://doi.org/10.31875/2410-2199.2025.12.02

[5] Dingxin Zhang and Ding Ding Retrofitting. Sunspaces in Qinghai-Tibet PlateauVernacular Dwellings: A Mini Review of Solar Gain Enhancement Strategies and Cultural Preservation Challenges. Journal of Solar Energy Research

Updates, 2025, 12, 30-41.
https://doi.org/10.31875/2410-2199.2025.12.03

[6] Impact of Solar Peak Energy and Weather Classification on BiLSTM-Based Solar Irradiance Forecasting in Equatorial Regions. Lek Keng Lim, Wai Shin Ho*, Haslenda Hashim and Zarina Ab Muis. Journal of Solar Energy Research Updates, 2025, 12, 103-115.
https://doi.org/10.31875/2410-2199.2025.12.08

[7] Battery-Integrated LED TV with Smart Power Management for Panel Protection and Voltage Stabilization. Md Rayhan Tanvir. American Journal of Electrical and Computer Engineering, 2025, Volume 14, Issue 5, 88-101.
https://doi.org/10.11648/j.epes.20251405.11

[8] A review of the technical-economic analysis of personal electric vehicle integration in the MENA region. Saida Karmich, Mohamed El Malki, Mohamed Maaouane, El Mostafa Ziani, Jamal Bouchnaif, Mourad Arabi. International Journal of Power Electronics and Drive System (IJPEDS), 2024, Vol. 16 No. 1 pp. 584 598.
https://doi.org/10.11591/ijpeds.v16.i1.pp584-598

[9] Performance Evaluation of Photovoltaic/Thermal (PV/T) System Using Different Design Configurations M. Imtiaz Hussain and Jun-Tae Kim. Sustainability, 2020, 12(22), 9520.
https://doi.org/10.3390/su12229520

[10] Optimal Control of Hybrid Photovoltaic/Thermal Water System in Solar Panels Using the Linear Parameter Varying Approach. Faycel Jamaaoui, Vicenç Puig, and Mounir Ayadi. Processes 2023, 11, 3426.
https://doi.org/10.3390/pr11123426

[11] Chaikovskaya E. (2024). Book. Smart Grid Technologies in Electric Systems for Wind and Solar Energy. Energy Science, Engineering and Technology. ISBN: 979-8-89113-446-1. Published by NOVA Science Publishers Inc. New York. P.156.

https://doi.org/10.31875/2410-2199.2025.12.11